Cross-linked chitosan/liposome hybrid system for the intestinal delivery of quercetin

Carla Caddeo[1,*], Octavio Díez-Sales[2,3], Ramon Pons[4], Claudia Carbone[5], Guido Ennas[6], Giovanni Puglisi[5], Anna Maria Fadda[1], Maria Manconi[1]

[1] Dept. of Scienze della Vita e dell'Ambiente, Sezione di Scienze del Farmaco, University of Cagliari, Via Ospedale 72, 09124 Cagliari, Italy

[2] Dept. of Pharmacy and Pharmaceutical Technology, University of Valencia, Avda Vicente Andrés Estellés s/n, 46100-Burjassot, Valencia, Spain

[3] Instituto de Reconocimiento Molecular y Desarrollo Tecnológico, Centro Mixto Universidad Politécnica de Valencia-Universidad de Valencia, Spain

[4] Dept. Tecnologia Química i de Tensioactius, Institut de Química Avançada de Catalunya (IQAC-CSIC) 08034 Barcelona, Spain

[5] Dept. of Scienze del Farmaco, University of Catania, Viale A. Doria 6, 95125 Catania, Italy

[6] Dept. of Scienze Chimiche e Geologiche, University of Cagliari, & Unità di Ricerca del Consorzio Nazionale di Scienze e Tecnologie dei Materiali (INSTM), Cittadella Universitaria di Monserrato, SS 554 bivio Sestu, 09042 Monserrato (CA), Italy

* Corresponding author:

Carla Caddeo, PhD

Dept. of Scienze della Vita e dell'Ambiente, Sezione di Scienze del Farmaco, University of Cagliari, Via Ospedale 72, 09124 Cagliari, Italy

Tel.: +39 0706758582; fax: +39 0706758553.

E-mail address: caddeoc@unica.it

Abstract

Quercetin is a flavonoid with antioxidant/anti-inflammatory properties, poorly absorbed when administered orally. To increase its bioavailability and optimize its release in the intestine, a hybrid system made of liposomes coated with cross-linked chitosan, named TPP-chitosomes, was developed and characterized by light scattering, transmission electron microscopy, differential scanning calorimetry, X-ray powder diffraction and Turbiscan® technology. The TPP-chitosomes were nanosized (~180 nm), fairly spherical in shape and unilamellar. The actual coating of the surface of liposomes with the cross-linked chitosan was demonstrated by Small-Angle X-ray Scattering.

The release of quercetin in simulated gastric and intestinal pH was investigated, the results showing that the system provided resistance to acidic conditions, and promoted the release in alkaline pH, mimicking the intestinal environment.

The proposed hybrid system represents a promising combination of nanovesicles and chitosan for the delivery of quercetin to the intestine in the therapy of oxidative stress/inflammation related disorders.

Keywords: quercetin; chitosan; liposomes; intestinal delivery

1. Introduction

Quercetin (3,3',4',5,7-pentahydroxyflavone) is a flavonoid present in a large number of edible vegetables and fruits [1,2]. This molecule has many health-promoting effects, including improvement of cardiovascular health, reducing risk for cancer, and coping with inflammatory disorders, mainly related to its strong antioxidant action, by which it upregulates the endogenous free radical defenses [3,4]. However, the efficacy of quercetin is limited due to its hydrophobicity, instability in physiological media, poor gastrointestinal absorption, and extensive xenobiotic metabolism at intestines and liver (i.e., glucuronidation or sulfation), which collectively contribute to its low oral bioavailability [4-6,7]. Various nanotechnological approaches have been used to enhance its solubility, dissolution rate, and hence, bioavailability, including solid dispersions, nanosuspensions, microemulsions, solid lipid nanoparticles and prodrugs [8-12]. Therefore, a critical need exists to develop alternative formulative strategies to overcome the shortcomings of quercetin and enhance its bioavailability.

The objective of this study was to develop, optimize and thoroughly characterize a formulation that enhances quercetin local bioavailability, bypasses the stomach and allows its release in the intestine for the treatment of disorders in which oxidative stress and inflammation are involved [2,13,14]. Among the different approaches to achieve intestinal drug delivery, the use of natural polymers holds promise. In recent years, polymer-coated liposomes have been proposed for the targeted delivery of drugs to the inflamed intestinal mucosa, upon oral administration [14]. Conventional liposomes can be hardly used, due to their low resistance to gastric pH and enzymatic degradation, but they can be easily protected by a polymeric coating. Chitosan is one of the most widely used polymers for coating liposomes. It is a linear cationic polysaccharide comprised of (1→4)-linked units of glucosamine and N-acetyl-glucosamine, mainly produced by partial deacetylation of chitin. Due to its unique and attractive properties, including biocompatibility, biodegradability, biorenewability and bioadhesion, chitosan is widely explored for biopharmaceutical applications,

especially for intestinal drug delivery [15,16]. However, it has a limited capacity for controlling drug release from oral dosage forms due to its fast dissolution in the stomach. To overcome this disadvantage, three dimensional networks have been developed by non-covalent complexation relying on electrostatic, hydrophobic and/or hydrogen bonding forces. The cationic amino groups of the repeating glucosamine units of chitosan can interact electrostatically with the anionic groups of other polyions to form polyelectrolyte complexes. These cross-linking interactions are physical in nature and reversible, but can provide the required properties for optimal drug delivery if the polymer is properly complexed. In a previous work, chitosan was complexed with Nutriose FM06®, a branched dextrin obtained from starch, and used to coat polyethylene glycol-containing vesicles, with the aim of producing an enzyme-sensitive, prebiotic, delayed release system for the delivery of quercetin to inflamed colon [14].

In the present paper, chitosan was complexed with sodium tripolyphosphate and used to coat liposomes, thus obtaining a hybrid system conceived for increasing the bioavailability of incorporated quercetin and optimizing its release rate to reach the intestine. To achieve these goals, it was imperative to assess the effectiveness and feasibility of the system by a thorough characterization using different analytical tools, such as Light Scattering, Transmission Electron Microscopy (TEM), Differential Scanning Calorimetry (DSC), X-Ray Powder Diffraction (XRPD), and Small-Angle X-ray Scattering (SAXS). Further, the ability of the system to release quercetin in simulated gastric and intestinal pH was investigated.

2. Materials and methods

2.1. Materials

Phospholipon90H and Phospholipon50 (P90H and P50; phosphatidylcholine-based phospholipids) were purchased from Lipoid GmbH (Ludwigshafen, Germany). Cholesterol (CHOL), chitosan of low molecular weight (50-190 kDa; degree of deacetylation ≥75%), sodium tripolyphosphate

(TPP), phosphate buffered saline (PBS, pH 7.4) and quercetin (QUE) were purchased from Sigma-Aldrich (Milan, Italy).

2.2. Preparation of TPP-chitosan/liposome hybrid system

P90H (60 mg/ml), P50 (30 mg/ml), CHOL (2 mg/ml) and quercetin (5 mg/ml) were weighed in a glass vial, PBS was added and the dispersion was sonicated (5 seconds on and 2 seconds off, 25 cycles) to obtain liposomes. After that, an equal volume of chitosan dispersion (0.5% w/v) in acetic acid/water (0.5 % v/v) was added to the vesicle dispersion to produce chitosomes, which were further treated with an equal volume of a TPP aqueous solution (0.2% w/v) to cross-link the chitosan, thus obtaining TPP-chitosomes.

2.3. Hybrid system characterization

The shape and morphology of liposomes, chitosomes and TPP-chitosomes were examined by TEM. Samples were stained with 1% phosphotungstic acid and examined with a JEM-1010 microscope (Jeol Europe, Paris, France) equipped with a digital camera MegaView III and the software "AnalySIS", at an accelerating voltage of 80 kV.

The average diameter, polydispersity index (P.I., a measure of the width of size distribution) and zeta potential of the systems were determined by Dynamic and Electrophoretic Light Scattering (DLS) using a Zetasizer nano-ZS (Malvern Instruments, UK). Samples (n = 6) were diluted with PBS (1:100) and analyzed at 25 °C.

The systems were purified from non-incorporated quercetin by dialysis. Each sample (1 ml) was loaded into Spectra/Por® tubing (12–14 kDa MW cut-off; Spectrum Laboratories Inc., DG Breda, The Netherlands) and dialyzed against PBS (2 l) for 2 hours, at room temperature. Both non-dialyzed and dialyzed samples were diluted with methanol (1:100) and assayed by HPLC to quantify the content of quercetin in the vesicular systems. A Perkin Elmer® Series 200 HPLC

equipped with a fluorescence detector was used; the column was a Kromasil® C18, 5.0 μm (150 cm × 4.6 mm); the mobile phase consisted of acetonitrile : water : acetic acid (80:19.8:0.2 v/v), eluted at a flow rate of 1 ml/min. Quercetin was excited at 370 nm and detected at 530 nm. The drug entrapment efficiency (EE%; Eq. 1) of the three systems was calculated as follows:

$$EE\% = \left(\frac{actual\ \ QUE}{initial\ \ QUE} \right) x100 \quad \text{(Eq. 1)}$$

where *actual QUE* is the amount of drug in vesicles after dialysis, and *initial QUE* is the amount of drug before dialysis, as calculated by HPLC.

X-ray powder diffractograms of the raw materials (i.e., P90H, P50, cholesterol, TPP, quercetin, chitosan), physical mixture and lyophilized drug-loaded TPP-chitosomes were recorded by a Bruker AXS D8 Advance, with CuKα radiation, equipped with a LynxEye energy-dispersive 1D detector (Karlsruhe, Germany) in the 2θ range from 8 to 80°, with steps of 0.02°.

DSC thermograms of the raw materials, physical mixture and lyophilized quercetin-loaded hybrid system were recorded using a DSC Mettler Toledo model 821 (Greifensee, Switzerland). Samples (2–5 mg) were scanned in sealed aluminum pans under nitrogen atmosphere. DSC thermograms were scanned at a constant rate of 10 °C/min, in a temperature range of 25-400 °C.

2.4. Small Angle X-ray Scattering

The nanostructure of the hybrid vesicle/polymer systems was studied by SAXS. SAXS patterns were recorded using a S3-MICRO (Hecus X-ray systems, Graz, Austria) coupled to a GENIX-Fox 3D X-ray source (Xenocs, Grenoble, France) working at 50 Kv and 1 mA. This source produces a focused X-ray beam with λ =1.542 Å at Cu Kα-line with more than 97% purity and less than 0.3% Kβ. The two detectors are position sensitive detectors PSD 50 (Hecus, Graz, Austria). The working q range were $0.01 \leq q \leq 0.6$ Å^{-1}, where $q = (4 \pi \sin\theta)/\lambda$ is the modulus of the scattering wave vector, θ the scattering angle and λ the wavelength. The samples were loaded in flow through glass

capillaries and the diffraction patterns were recorded at 25 °C. For each experiment, the scattering pattern was recorded as a sum of subscans to verify there was no sample evolution. The scattering curves were background subtracted using the same capillary filled with water. To obtain useful information from the scattering curves, a home-made minimization routine based on the Leverberg-Marquad scheme was used. The calculated scattering curves were smeared according to our experimental set up, which corresponded to a detector focused beam convoluted with the linear detector width. We used a model based on the one developed by Pabst et al. [17] to calculate the bilayer electronic profile and its combination with the Caillé structure factor. Contrary to the model of Pabst, we also included a constant term through the hydrophobic part of the bilayer, to give account of the methylene contribution [18]. Further, in order to simulate asymmetric profiles, the description of Varga et al. [19] for the bilayer electronic density was used. In this case, we restricted the possible free parameters by allowing only the intensity to be different in both bilayers.

2.5. Accelerated stability studies

The stability of quercetin hybrid systems was evaluated by standard long-term stability tests, i.e. analyzing vesicle mean size, P.I. and zeta potential over one month at 4 °C. Accelerated stability tests were also carried out by using the Turbiscan® AG Station (Formulaction, l'Union, France), which was previously used to evaluate the stability of colloidal dispersions [20]. The apparatus consists in the Turbiscan Lab Expert, which measures the multiple dispersion of the light by suspensions, coupled with an Aging Station constituted by a robot with three thermoregulated blocks for the storage of the samples. 10 ml of each sample was placed in a glass cell in the Turbiscan block and kept at 25 and 40 °C for 15 days. The detection head is composed of a pulsed near-infrared light source (λ = 850 nm), a transmission (T) and a backscattering (BS) detector. The former receives the light that crosses the sample (at 180° from the incident beam), while the latter receives the light scattered backwards by the sample (at 45° from the incident beam). The

measurement principle of the Turbiscan® is based on multiple light scattering: the photons are scattered many times by the particles before being detected by the backscattering detector. The detection head scans the height of the sample cell, acquiring transmitted and backscattered light each 40 μm. The intensity of the light backscattered by the sample depends on three parameters: the diameter of the particles, their volume fraction and the relative refractive index between the dispersed and continuous phases. Therefore, any change due to a variation of the particle size (flocculation, coalescence) or a local variation of the volume fraction (migration phenomena: creaming, sedimentation) is detected by the optical device. The Turbiscan® makes scans at various pre-programmed times and overlays the profiles on one graph, in order to show possible destabilization phenomena. In our experiments, the stability of the samples was evaluated on the basis of the variation of transmission (ΔT), which was elaborated as ΔT profiles by the Turbiscan EasySoft Converter showing ΔT in ordinate and the height of the cell in abscissa.

For a comparative evaluation between the different samples we exploited the Turbiscan Stability Index (TSI) computation, that provides a key number related to the general behaviour of the formulation. Samples were significantly different for ΔTSI values greater than 0.4.

2.6. In vitro drug release studies

The *in vitro* release profile of quercetin from the vesicle dispersions was assessed in two different buffered solutions mimicking the gastric and intestinal pH (1.2 and 7.0, respectively), using a USP basket dissolution apparatus. The dispersions were loaded in a dialysis tube (see Section 2.3) and immersed in the dissolution medium, thermostated at 37.0 ± 0.5 °C. Drug release was assessed: for 120 min (2 h) at pH 1.2 and for 480 min (8 h) at pH 7.0. At scheduled time intervals, an aliquot of the medium was withdrawn and refreshed to ensure sink conditions, and the drug content was assayed by HPLC (see Section 2.3). All experiments were performed in triplicate.

2.7. Statistical analysis of data

Results are expressed as the mean ± standard deviation (SD). Multiple comparison of means (Tukey's test) was used to substantiate statistical differences between groups, while Student's t-test was used to compare two samples. Significance was tested at the 0.05 level of probability (*p*). Data analysis was carried out with the software package R, version 3.1.2.

3. Results and discussion

3.1. Hybrid system's fabrication and key features

A hybrid system made of quercetin-loaded liposomes coated with TPP cross-linked chitosan was developed aiming at realizing an efficient intestinal delivery system by exploiting the attractive biopharmaceutical properties of the flavonoid, the phospholipid vesicles, and the polymer, as well.

The polycationic chitosan was dissolved in acetic acid solution to protonate the free amino groups and allow the supramolecular self-organizing interaction with negatively charged liposomes on the one hand, and with negatively charged polyanion TPP, acting as a crosslinker, on the other. Hence, a three-dimensional polyelectrolyte coating was formed on the surface of liposomes, with the aim of protecting quercetin from the gastric environment and controlling its release to reach the intestine.

The cross-linked chitosan/liposome hybrid system was thoroughly characterized by evaluating key parameters, also in comparison with the native liposomes and the chitosan-only coated liposomes.

The morphological investigation of quercetin liposomes by TEM showed small vesicles varying from spherical to elongated, irregular shape. The liposome membrane was composed of two or more lamellae, thus resulting in oligolamellar structures (Fig. 1A). Chitosomes and TPP-chitosomes displayed similar characteristics: they were larger than liposomes, quasi-spherical shaped, and their lamellar arrangement was not detectable (Fig. 1B). No drug crystals were visible on TEM images, regardless of the step of processing.

In agreement with TEM observations, DLS results (Table 1) showed that all the three systems prepared were nanosized, being around 120 nm when the quercetin was not loaded, around 140 nm when the quercetin was loaded in liposomes, and even larger (180 nm; $p < 0.05$) when the vesicles were coated with chitosan and TPP-chitosan. The P.I. was around 0.4 for all the three systems, indicating an acceptable degree of polydispersity. The zeta potential of liposomes was negative (~ -30 mV; Table 1), due to the charge carried by P90H and P50, which is ideal for binding positively charged chitosan. An inversion of the zeta potential was detected upon coating the liposomes with the polymer (+46 mV), and as soon as the cross-linking with anionic TPP took place, the zeta potential became less positive, approaching neutrality (+2 mV). These results confirm that cross-linked chitosan formed a shell layer on the outer surface of liposomes, which is expected to protect the inner phospholipid structure and the incorporated quercetin.

The entrapment efficiency (EE%; Table 1) of quercetin in liposomes was 55%, and it was clearly affected by the chitosan coating, as it increased to 70% and 91%. This is reasonably due to the fact that the free quercetin, which was not entrapped in liposomes, was embedded in the three-dimensional polyelectrolyte shell during the coating and cross-linking process.

3.2. SAXS analysis

Further insights into the morphology and lamellar arrangement of the prepared liposomes, as well as the effect of the polymer coating and cross-linking, were gained by SAXS, a well established technique for the study of self-assembling nanostructures.

The SAXS curve of empty liposomes showed the typical shape for unilamellar vesicles, that is a broad symmetric band (Fig. 2A). The coating with chitosan and the cross-linking with TPP did not alter such arrangement, as demonstrated by the similar SAXS profiles (Fig. 2A). On the other hand, the presence of quercetin had a moderate effect on the three systems, the most evident being a

conformational difference in liposomes, as the scattering curve featured two bumps, which can be attributed to vesicle oligolamellarity (Fig. 2C).

All the SAXS patterns were fitted with two models, one for the symmetric and the other for the asymmetric bilayer, and the fitting parameters are reported in Table 2. For liposomes, both the models provided an adequate fitting of the scattering curves, as it can be deduced from the slight difference in χ^2_{red}, being approximately 2 (for purely statistical noise $\chi^2_{red} = 1$; for good statistical fitting $\chi^2_{red} < 3$; χ^2_{red} in the range of 5 to 10 = poor fitting). In contrast, the differences in χ^2_{red} were significant for the chitosomes, and even more pronounced for TPP-chitosomes (~30 vs 2; Table 2), pointing to the superiority of the asymmetric model for the fitting of the hybrid systems.

In order to minimize the fitted parameters, in the asymmetric model we allowed the intensity of the external Gaussian to be different from that of the inner Gaussian, preserving both the width and position with respect to the bilayer center. It is quite clear from the data summarized in Table 2 that chitosan was arranged on the outer surface of liposomes and TPP was entangled with the chitosan chains. Indeed, the main effect of chitosan was a reduction of the polar heads separation, with an increase in width of the Gaussians corresponding to the polar heads (σ_h; Table 2). Further, proceeding from liposomes, which were symmetric or slightly asymmetric, with the interior layer more dense than the outer layer (ρ_h vs ρ_{h2}), to chitosomes, the outer polar head electron density increased, and this was even more noticeable for TPP-chitosomes (ρ_{h2}, Table 2; Fig. 2B and D). Additionally, Z_h, which is the distance of the polar heads to the centre of the bilayer, increased for liposomes when the quercetin was loaded, suggesting an enlargement of the vesicles. This is consistent with the DLS results showing that the mean diameter of liposomes increased from 116 to 138 nm (Table 1). Such increase in Z_h was not observed for the hybrid systems, despite the increase in size measured by DLS (from 120 to 180 nm). This confirms the chitosan did not alter the assembly of the phospholipids in vesicles, but was rather arranged on the outer surface of liposomes

forming a three-dimensional shell when cross-linked with TPP, which caused the enlargement detected by DLS.

3.3. X-ray diffraction and DSC analyses

X-ray diffraction studies were carried out to investigate the microstructure of the drug, the phospholipids and the polymer and their interactions in the prepared hybrid system (Fig. 3). The raw P90H showed partially crystalline characteristics, with the major peak at approximately 21° 2θ, while P50 showed amorphous structure. Cholesterol exhibited several sharp crystal reflections [21], TPP was in the monoclinic crystalline phase C2/c (a=16.0, b=5.24, c=11.25 Å, β=93°) [22], and quercetin revealed its anhydrous crystalline form, with multiple sharp peaks of different intensities between 8° and 32° 2θ [23]. Chitosan exhibited two major peaks at around 13° and 19° 2θ, the first one showing stronger intensity, which correspond to the α and β crystal forms and represent the typical fingerprints of the semi-crystalline polymer [13,24].

For comparative purposes, a physical mixture of the raw components was prepared by gently grinding the powders at the same mass ratio as in TPP-chitosomes. The diffractogram of the physical mixture was basically a superimposition of the individual patterns of the main components, the phospholipids and chitosan (the two amorphous halos were clearly visible), hiding the peaks characterizing quercetin, and there was no sign of the formation of a new structure.

On the other hand, the diffractogram of the TPP-chitosomes exhibited a distinctive pattern, with two predominant low-intensity, broad peaks, indicating the structural changes of the components, and the presence of chemical interactions between crosslinked-chitosan, quercetin and the phospholipid vesicle when they formed the hybrid system. In addition, the high-intensity crystalline peaks of quercetin were not detectable, suggesting its amorphization/dispersion when loaded in TPP-chitosomes.

DSC thermal analyses of the raw materials, their physical mixture and quercetin-loaded TPP-chitosomes are presented in Fig. 4. In the thermogram of P90H, a major endothermic peak was detected at 82 °C, while for P50 a set of thermal events was observed between 110 and 295 °C. This may be due to the fact that P90H is composed mostly of phosphatidylcholine (not less than 90%), which reflects in the major melting peak, while P50 contains 45% phosphatidylcholine plus 10–18% phosphatidylethanolamine, and triglycerides and lipids (e.g., fatty acids, glycolipids, phosphatidylinositol), each one having a different melting point [25].

The thermogram of cholesterol showed a sharp endothermic peak at 149 °C, corresponding to its melting point, and the curve of TPP displayed three major endothermic peaks at 81, 194 and 295 °C. The thermogram of chitosan was characterized by two thermal events: the first endothermic centred at about 45 °C, attributed to the loss of water associated with the hydrophilic groups of the polymer, and the second exothermic centred at about 309 °C, corresponding to the thermal degradation of the polymer. The thermogram of quercetin displayed a major sharp endothermic peak at 322 °C, which corresponds to the melting point of the drug crystals. This peak was still detectable in the curve of the physical mixture, which was an apparent combination of events of the phospholipids and chitosan. In contrast, the DSC curve of the TPP-chitosomes showed the complete disappearance of the characteristic peak of quercetin, suggesting that it may be molecularly dispersed within the phospholipid-polymer system. Further, the DSC profile was markedly different from that of the physical mixture, showing broad signals with low intensity, which may be ascribed to the presence of physical or chemical interactions in a newly formed system.

3.4. Accelerated stability tests

The Turbiscan® technology was exploited to detect possible instability phenomena in the prepared systems, thus providing an accurate, qualitative description of the vesicular dispersions, in terms of demixing behavior and predictive stability. No variation in vesicle size occurred for liposomes

stored at 20 and 40 °C for 15 days, since the transmission profile was within the interval ±2% (Fig. 5). On the other hand, TPP-chitosomes showed a certain instability due to the vesicle migration to the top of the cuvette, indicating the occurrence of creaming. The intensity of the phenomenon was higher for TPP-chitosomes than for chitosomes, as shown in the ΔT profiles. However, creaming is a reversible phenomenon, since the creamed layer can be easily redispersed by gentle shaking.

On the basis of the TSI results (Fig. 5), the following stability order can be derived: chitosomes ≥ liposomes > TPP-chitosomes. These findings are in accordance with the stability profiles observed at 24 h for chitosan-coated liposomes by Gonçalves et al. [26], and highlight the important role of chitosan in the structural organization of the nanosystem, that is an improvement of the stability. These findings are in agreement with the DLS data, and can be related to the zeta potential values of the samples. The zeta potential is a well-known, useful tool to predict the sample stability during storage, ensured by electrostatic repulsion. When the particles have and maintain a large negative or positive zeta potential, like in liposomes (-32 mV) and chitosomes (+46 mV), they repel each other and the dispersion is stable. In particles with low zeta potential, like in TPP-chitosomes (+2 mV), there is only a little repulsion force and the particles will eventually aggregate, resulting in dispersion instability. Overall, it can be inferred that chitosan and TPP critically modified the sample stability, with an opposite effect likely correlated with the modification of the surface charge of the hybrid system, in accordance with previous findings on the stability enhancement of lipid nanoparticles due to the addition of a positively charged coating layer [20]. Nevertheless, as mentioned above, it is worth noting that the instability of TPP-chitosomes was reversible, as the creamed layer could be easily redispersed by gentle shaking.

3.5. In vitro drug release studies

The ability of the prepared hybrid system to pass through the acidic environment of the stomach and release the incorporated quercetin in the intestine was assessed by conducting drug release studies

under conditions mimicking the stomach and intestine environment. The release profiles of quercetin from TPP-chitosomes are shown in Fig. 6, as a function of the time and pH of the release medium. At acidic pH, the release of quercetin from TPP-chitosomes was not time-dependent, reached the maximum amount after 10 minutes, and remained constant up to 2 h. Conversely, at intestinal pH, the release was enhanced and time-dependent: after 2 h the amount of drug released was 2 times greater than that obtained at pH 1.2, and after 8 h it was 2.7-fold greater. Therefore, it can be concluded that the system modulated the release in a pH-dependent fashion. Further, the observed sustained release may be attributed to the diffusion of quercetin through the hybrid system.

4. Conclusions

The goal of this work was to design a formulation for the intestinal delivery of quercetin, with great potential for health promotion. The development of such system that achieves both therapeutic effectiveness and biocompatibility is a challenging task, since quercetin has low oral bioavailability. In this context, a cross-linked chitosan/liposome hybrid nanosystem loading quercetin was successfully fabricated, without any complicated apparatus or organic solvents. The morphology and structure of the system were analysed using different non-invasive techniques, such as light scattering, transmission electron microscopy, differential scanning calorimetry and X-ray powder diffraction. The system possessed a satisfactory size range (~180 nm) and attractive entrapment efficiency (~91%). The formation of a cross-linked, coating layer on the liposome surface, as well as the effect of the polymer-mediated conformational change were followed with the help of SAXS technique and explained with a proposed model, representing a novel aspect of this work. Indeed, it was demonstrated that chitosan did not alter the assembly of the phospholipids in vesicles, but was rather arranged on the outer surface of liposomes forming a three-dimensional shell when cross-linked with TPP, which caused an increase in size of the system.

The use of a protective three-dimensional polyelectrolyte shell layer was expected to allow circumventing possible damage of both the vesicles and the incorporated drug due to the acidic pH of the stomach. From *in vitro* tests, it was found that the system modulated the release of quercetin as a function of the pH (preferably alkaline), and it was likely governed by the diffusion of the drug through the hybrid system.

In conclusion, several insights to understand the structure of the hybrid system and its potential as smart carrier in drug delivery applications, especially for the therapy of intestinal inflammatory-based disorders, were given. We anticipate that this study would provide a better understanding of the advantages of combining liposomes and chitosan, paving the way for the next investigations that will be carried out on the proposed system, by changing the amount of both the quercetin and the polymer, to confirm the obtained results and to model the release properties of the system. Further studies are also required to evaluate the fate and the therapeutic efficacy of the hybrid system *in vivo*, upon oral administration.

Acknowledgements

Dr. Pons acknowledges financial support from MINECO-CTQ2013-41514-P.

References

[1] Caddeo, C., Díez-Sales, O., Pons, R., Fernàndez-Busquets, X., Fadda, A.M., & Manconi, M. (2014). Topical anti-inflammatory potential of quercetin in lipid-based nanosystems: in vivo and in vitro evaluation. *Pharmaceutical Research, 31,* 959–968.

[2] Singhal, A., Hain, J., Singhal, V., Elias, E.J., & Showkat, A. (2011). Colon-targeted quercetin delivery using natural polymer to enhance its bioavailability. *Pharmacognosy Research, 3,* 35-39.

[3] Boots, A.W., Haenen, G.R., & Bast, A. (2008). Health effect of quercetin: from antioxidant to nutraceutical. *European Journal of Pharmacology, 585,* 325-337.

[4] Tran, T.H., Guo, Y., Song, D., Bruno, R.S., & Lu, X. (2014). Quercetin-containing self-nanoemulsifying drug delivery system for improving oral bioavailability. *Journal of Pharmaceutical Sciences, 103,* 840–852.

[5] Dian, L., Yu, E., Chen, X., Wen, X., Zhang, Z., Qin, L., Wang, Q., Li, G., & Wu, C. (2014). Enhancing oral bioavailability of quercetin using novel soluplus polymeric micelles. *Nanoscale Research Letters, 9,* 684.

[6] Ratnam, D.V., Ankola, D.D., Bhardwaj, V., Sahana, D.K., & Kumar, M.N. (2006). Role of antioxidants in prophylaxis and therapy: a pharmaceutical perspective. *Journal of Controlled Release, 113,* 189–207.

[7] Xu, G., Shi, H., Ren, L., Gou, H., Gong, D., Gao, X., & Huang, N. (2015). Enhancing the anti-colon cancer activity of quercetin by self-assembled micelles. *International Journal of Nanomedicine, 10,* 2051–2063.

[8] Gao, Y., Wang, Y., Ma, Y., Yu, A., Cai, F., Shao, W., & Zhai, G. (2009). Formulation optimization and in situ absorption in rat intestinal tract of quercetin loaded microemulsion. *Colloids and Surfaces B: Biointerfaces, 71,* 306–314.

[9] Gao, L., Liu, G., Wang, X., Liu, F., Xu, Y., & Ma, J. (2011). Preparation of a chemically stable quercetin formulation using nanosuspension technology. *International Journal of Pharmaceutics, 404*, 231–237.

[10] Kakran, M., Sahoo, N.G., & Li, L. (2011). Dissolution enhancement of quercetin through nanofabrication, complexation, and solid dispersion. *Colloids and Surfaces B: Biointerfaces, 88*, 121–171.

[11] Li, H., Zhao, X., Ma, Y., Zhai, G., Li, L., & Lou, H. (2009). Enhancement of gastrointestinal absorption of quercetin by solid lipid nanoparticles. *Journal of Controlled Release, 133*, 238–244.

[12] Montenegro, L., Carbone, C., Maniscalco, C., Lambusta, D., Nicolosi, G., Ventura, C.A., & Puglisi, G. (2007). In vitro evaluation of quercetin-3-o-acyl esters as topical prodrugs. *International Journal of Pharmaceutics, 336*, 257-262.

[13] Caddeo, C., Nácher, A., Díez-Sales, O., Merino-Sanjuán, M., Fadda, A.M., & Manconi, M. (2014). Chitosan–xanthan gum microparticle-based oral tablet for colon-targeted and sustained delivery of quercetin. *Journal of Microencapsulation, 31*, 694–699.

[14] Castangia, I., Nácher, A., Caddeo, C., Merino, V., Díez-Sales, O., Catalán-Latorre, A., Fernàndez-Busquets, X., Fadda, A.M., & Manconi, M. (2015). Therapeutic efficacy of quercetin enzyme-responsive nanovesicles for the treatment of experimental colitis in rats. *Acta Biomaterialia, 13*, 216–227.

[15] Bowman, K., & Leong, K.W. (2006). Chitosan nanoparticles for oral drug and gene delivery. *International Journal of Nanomedicine, 1*, 117–128.

[16] Gulbake, A., & Jain, S.K. (2012). Chitosan: a potential polymer for colon-specific drug delivery system. Expert Opinion on Drug Delivery, 9, 713-729.

[17] Pabst, G., Rappolt, M., Amenitsch, H., & Laggner, P. (2000). Structural information from multilamellar liposomes at full hydration: full q-range fitting with high quality x-ray data. *Physical Review E, 62*, 4000–4009.

[18] Caddeo, C., Chessa, M., Vassallo, A., Pons, R., Diez-Sales, O., Fadda, A.M., & Manconi, M. (2013). Extraction, purification and nanoformulation of natural phycocyanin (from Klamath algae) for dermal and deeper soft tissue delivery. *Journal of Biomedical Nanotechnology, 9,* 1929–1938.

[19] Varga, Z., Berényi, S., Szokol, B., Õrfi, L., Kéri, G., Peták, I., Hoell, A., & Bóta, A. (2010). A closer look at the structure of sterically stabilized liposomes: a Small-Angle X-ray Scattering study. *The Journal of Physical Chemistry B, 114*, 6850–6854.

[20] Carbone, C., Campisi, A., Manno, D., Serra, A., Spatuzza, M., Musumeci, T., Bonfanti, R., & Puglisi, G. (2014). The critical role of didodecyldimethylammonium bromide on physico-chemical, technological and biological properties of NLC. *Colloids and Surfaces B Biointerfaces, 121*, 1-10.

[21] Hsu, L.Y., Kampf, J.W., & Nordman, C.E. (2002). Structure and pseudosymmetry of cholesterol at 310 K. *Acta Crystallographica Section B, 58*, 260-264.

[22] Davies, D.R., & Corbridge, D.E.C. (1958). The crystal structure of sodium triphosphate, $Na_5P_3O_{10}$, Phase II. *Acta Crystallografica, 11*, 315-319.

[23] Filip, X., Grosu, I.G., Miclăuş, M., & Filip, C. (2013). NMR crystallography methods to probe complex hydrogen bonding networks: application to structure elucidation of anhydrous quercetin. *CrystEngComm, 15*, 4131-4142.

[24] Swain, S.K., Satyabrata, D., Kisku, S.K., & Singh, R.K. (2014). Thermal and oxygen barrier properties of chitosan bionanocomposites by reinforcement of calcium carbonate nanopowder. *Journal of Materials Science and Technology, 30*, 791-795.

[25] Caddeo, C., Valenti, D., Nácher, A., Manconi, M., & Fadda, A.M. (2015). Exploring the co-loading of lidocaine chemical forms in surfactant/phospholipid vesicles for improved skin delivery. *Journal of Pharmacy and Pharmacology, 67*, 909–917.

[26] Gonçalves, M.C., Mertins, O., Pohlmann, A.R., Silveira, N.P., & Guterres, S.S. (2012). Chitosan coated liposomes as an innovative nanocarrier for drugs. *Journal of Biomedical Nanotechnology, 8*, 240-250.

Captions to Figures

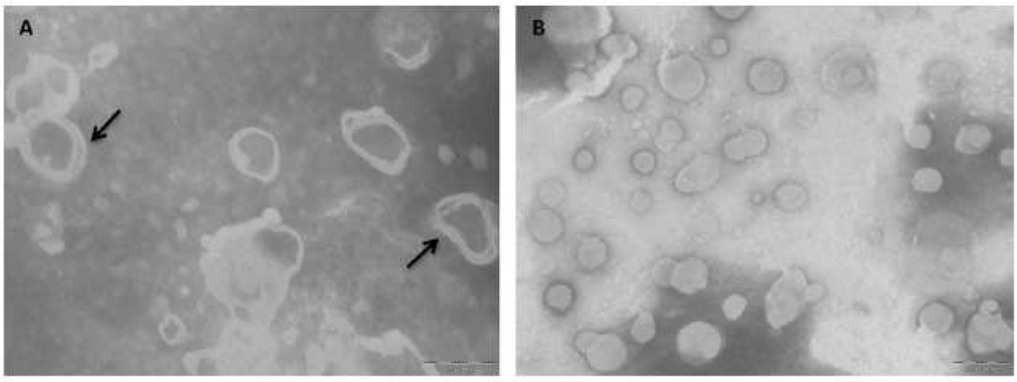

Fig. 1. TEM images of liposomes (A) and TPP-chitosomes (B). The arrows indicate the lamellae of liposomes.

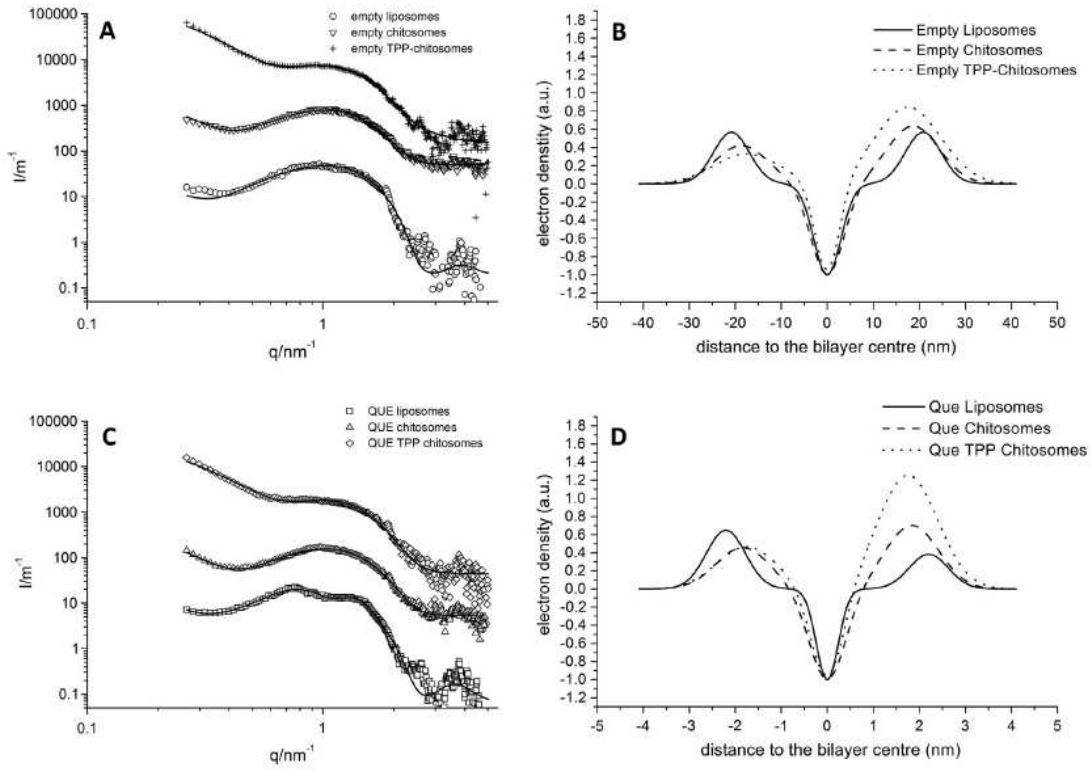

Fig. 2. SAXS (A-C) and electron density (B-D) profiles of empty and quercetin-loaded liposomes, chitosomes and TPP-chitosomes. The lines correspond to the best fits of Gaussian bilayer models: see the text for details on the fitting.

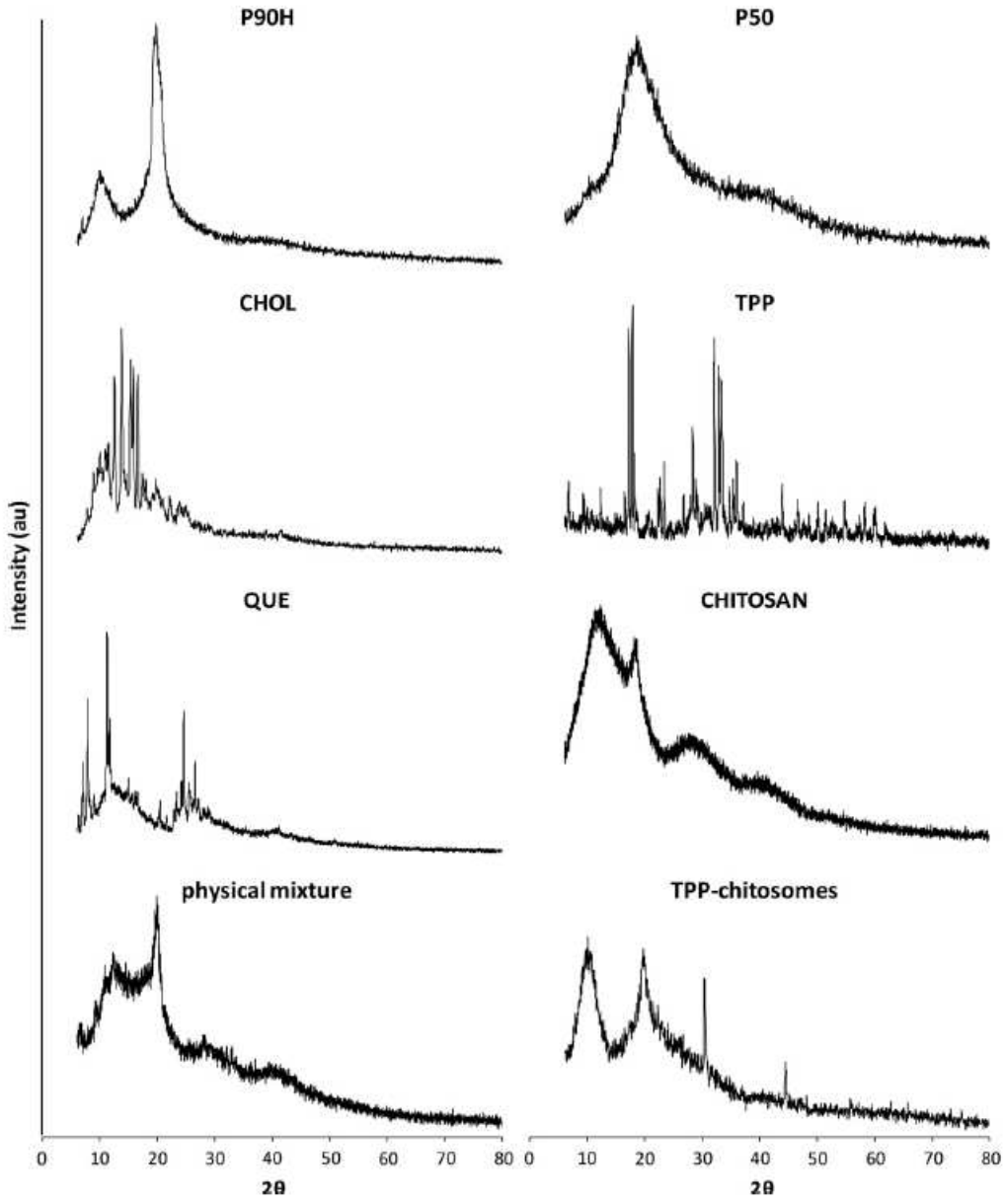

Fig. 3. X-ray diffractograms of raw components, physical mixture and TPP-chitosomes.

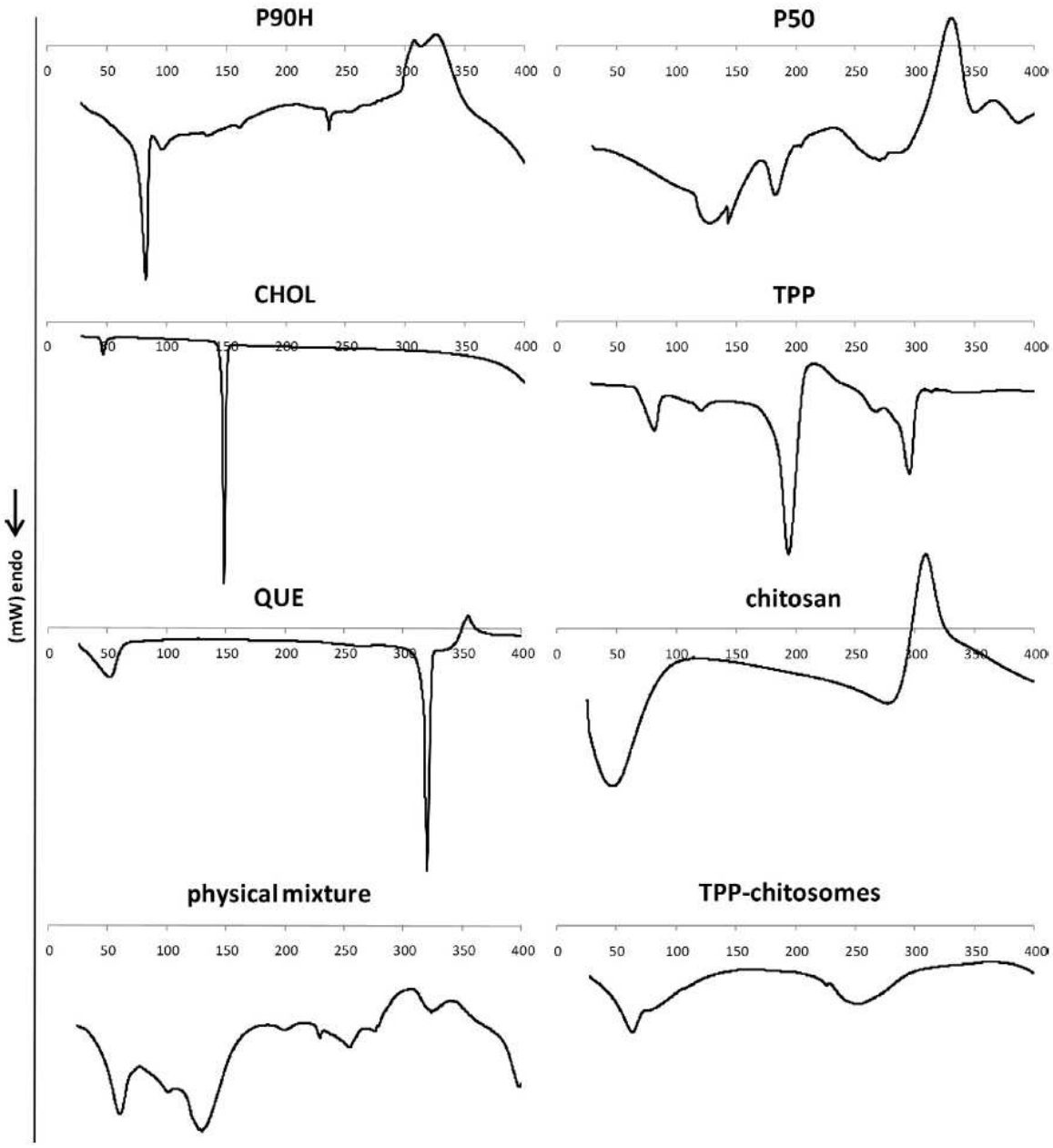

Fig. 4. DSC thermograms of raw components, physical mixture and TPP-chitosomes.

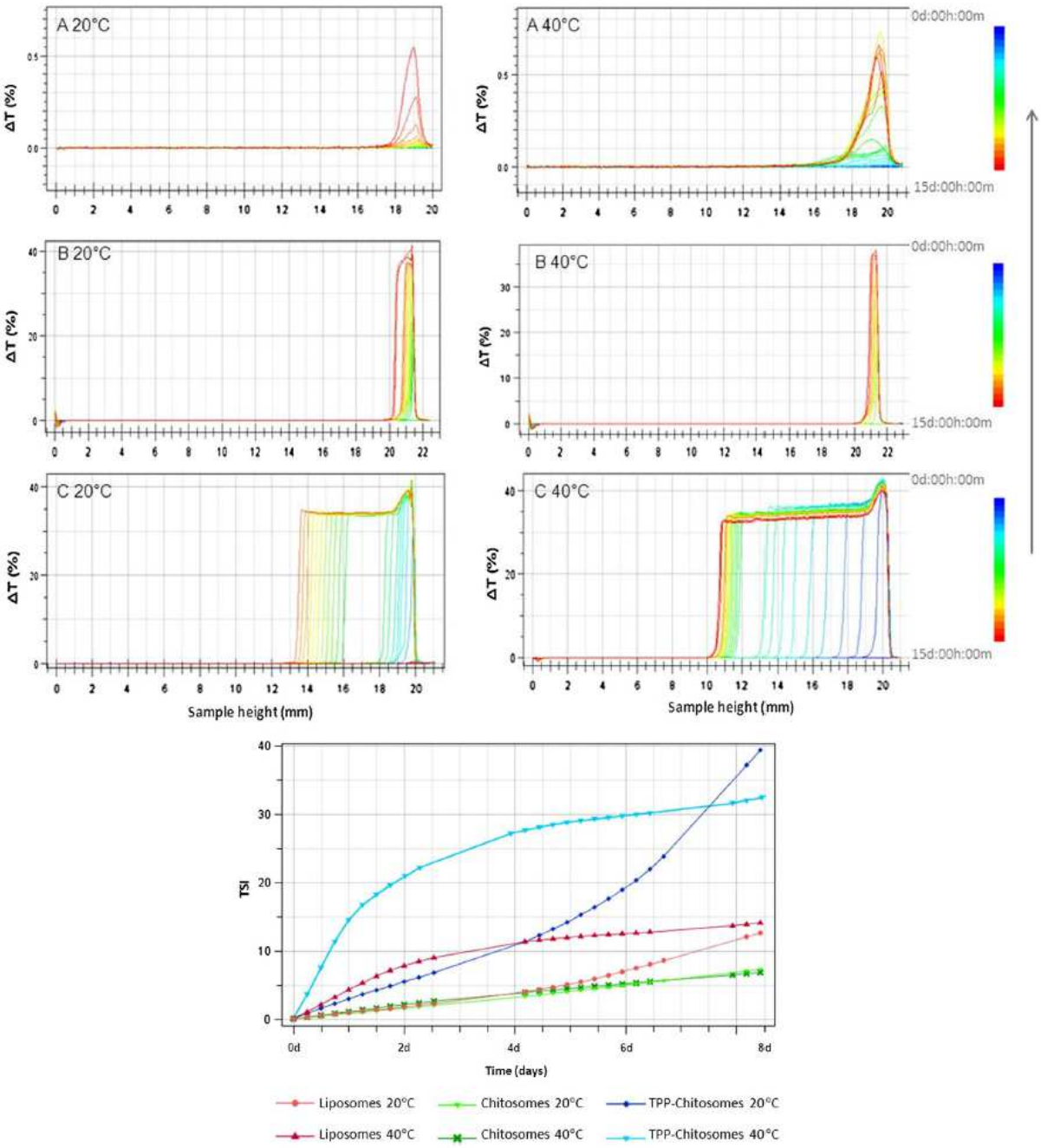

Fig. 5. Transmission profiles (ΔT) of liposomes (A), chitosomes (B) and TPP-chitosomes (C) stored at 20 and 40 °C. The data are represented as a function of time (0-15 days) and sample height (0 to 20 mm). The progression of the analysis over time is indicated by the arrow.

The Turbiscan stability index (TSI) of liposomes, chitosomes and TPP-chitosomes stored at 20 and 40 °C is also presented.

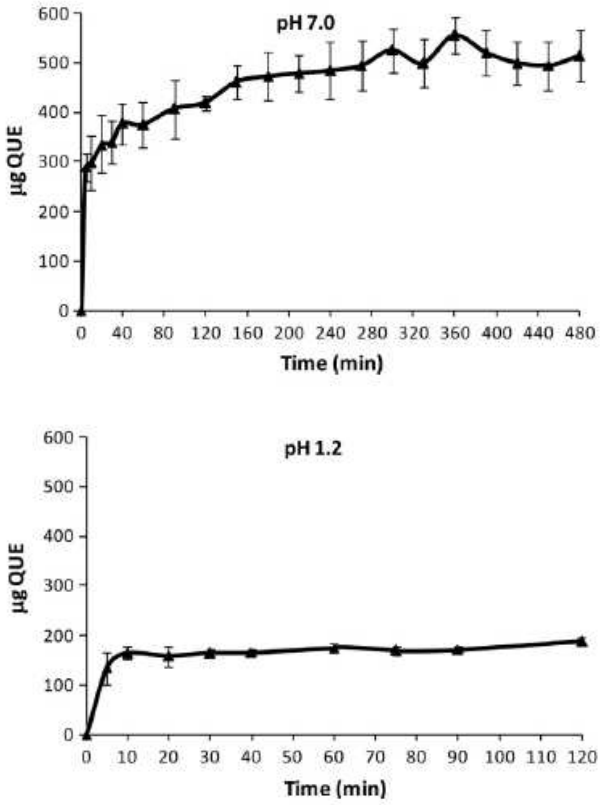

Fig. 6. Quercetin release from TPP-chitosomes over 2 hours at pH 1.2 and over 8 hours at pH 7.0, at 37 °C. Error bars represent standard deviation, n = 3.

Table 1

Main features of empty and quercetin-loaded systems: average size; polydispersity index, P.I.; zeta potential, ZP; entrapment efficiency, EE%. Values are the means ± standard deviation (n = 6).

	Size nm ± SD	P.I.[a]	ZP mV ± SD	EE%
Empty liposomes	116 ± 4.5	0.38	-20 ± 5.4	
Empty chitosomes	119 ± 2.0	0.44	+23 ± 9.3	
Empty TPP-chitosomes	120 ± 2.9	0.46	+1.6 ± 0.8	
QUE liposomes	138 ± 6.3	0.38	-32 ± 3.6	55 ± 7.0
QUE chitosomes	174 ± 5.1	0.39	+46 ± 9.3	70 ± 10.0
QUE TPP-chitosomes	182 ± 7.0	0.42	+2.3 ± 2.1	91 ± 1.0

a SD for P.I. values was always ≤0.02.

Table 2A. Comparison of the fitting parameters obtained from the symmetric (left column) and asymmetric (right column) models for the empty samples shown in figure 2.

	Liposomes		Chitosomes		TPP-chitosomes	
χ^2_{red} [1]	2.6	2.3	3.7	1.1	34.9	1.9
σ_h^2	5.5±0.5	5.6±0.5	5.8±0.5	8.0±0.5	1.3±0.5	10.1 ±0.5
ρ_h [3]	0.57±0.03	0.49±0.05	0.37±0.04	0.4±0.04	1. 7±0.2	0.3±0.08
Z_h [4]	20.8±1.0	20.8±1.0	20.6±1.0	18.7±1.0	16.0±2.0	17.5±1.0

σ_c[5]	4.2±0.5	4.0±0.5	3.1±0.5	5.1±0.5	8.8±1.0	3. 8±0.5
ρ_{h2}[6]		0.7±0.08		0.6±0.05		0.8±0.10

Table 2B. Comparison of the fitting parameters obtained from the symmetric (left column) and asymmetric (right column) models for the quercetin loaded samples shown in figure 2.

	Liposomes[7]		Chitosomes		TPP-chitosomes	
χ^2_{red}	2.4	1.9	6.4	1.07	30.6	2.7
σ_h	4.4±0.5	6.0±0.5	6.0±0.5	8.2±0.5	1.5±0.5	9.2±0.5
ρ_h	0.63±0.04	0.6±0.04	0.5±0.1	0.46±0.04	1.2±0.2	0.5±0.08
Z_h	22.4±1.0	22.0±1.0	20.3±1.0	18.4±1.0	15.9±2.0	17.5±1.0
σ_c	4.0±0.5	3.4±0.5	4.1±0.5	5.6±0.5	7.6±1	5.0±0.5
ρ_{h2}		0.4±0.07		0.70±0.05		1.3±0.15

[1] χ^2_{red} =1 for a perfectly statistical fit, values of 2 or 3 are reasonably good.
[2] σ_h corresponds to the polar head gaussian amplitude in Å.
[3] ρ_h corresponds to the polar head relative electron density (-1 for the methyl groups).
[4] Z_h the center of the polar head gausian with respect to the bilayer centre in Å.
[5] σ_c the methyl deep amplitude in Å.
[6] ρ_{h2} only appears for the assymetric model and corresponds to the outer polar head electron density.
[7] This sample showed significant multilamelarity, with a repetition distance of 81.1±0.5 Å, a Caillé paremeter of 0.25±0.02 and 1.5±0.2 correlated bilayers.